Gene coexpression patterns predict opiate-induced brain-state transitions

Julia K. Brynildsen[a], Kyla D. Mace[a], Eli J. Cornblath[b,c,d,e,f], Carmen Weidler[g], Fabio Pasqualetti[h], Danielle S. Bassett[b,c,d,e,f,i], and Julie A. Blendy[a,1]

[a]Department of Systems Pharmacology and Translational Therapeutics, Perelman School of Medicine, University of Pennsylvania, Philadelphia, PA 19104; [b]Department of Bioengineering, University of Pennsylvania, Philadelphia, PA 19104; [c]Department of Neurology, University of Pennsylvania, Philadelphia, PA 19104; [d]Department of Psychiatry, University of Pennsylvania, Philadelphia, PA 19104; [e]Department of Electrical & Systems Engineering, University of Pennsylvania, Philadelphia, PA 19104; [f]Department of Physics & Astronomy, University of Pennsylvania, Philadelphia, PA 19104; [g]Department of Psychiatry, Psychotherapy and Psychosomatics, Faculty of Medicine, RWTH Aachen University, 52074 Aachen, Germany; [h]Department of Mechanical Engineering, University of California, Riverside, CA 92521; and [i]Santa Fe Institute, Santa Fe, NM 87501

Edited by Olaf Sporns, Indiana University, Bloomington, IN, and accepted by Editorial Board Member Michael S. Gazzaniga June 24, 2020 (received for review February 25, 2020)

Opioid addiction is a chronic, relapsing disorder associated with persistent changes in brain plasticity. Reconfiguration of neuronal connectivity may explain heightened abuse liability in individuals with a history of chronic drug exposure. To characterize network-level changes in neuronal activity induced by chronic opiate exposure, we compared FOS expression in mice that are morphine-naïve, morphine-dependent, or have undergone 4 wk of withdrawal from chronic morphine exposure, relative to saline-exposed controls. Pairwise interregional correlations in FOS expression data were used to construct network models that reveal a persistent reduction in connectivity strength following opiate dependence. Further, we demonstrate that basal gene expression patterns are predictive of changes in FOS correlation networks in the morphine-dependent state. Finally, we determine that regions of the hippocampus, striatum, and midbrain are most influential in driving transitions between opiate-naïve and opiate-dependent brain states using a control theoretic approach. This study provides a framework for predicting the influence of specific therapeutic interventions on the state of the opiate-dependent brain.

opioid dependence | network analysis | mice | graph theory | control theory

Drug dependence and relapse liability are thought to be supported by lasting alterations in neural circuitry. In light of the ongoing opioid epidemic in the United States, there is growing interest in connectivity-based approaches to understand the influence of opioid use disorder (OUD) on the brain's responsiveness to opiates and opiate-related cues (1). Such approaches hold promise for identifying biomarkers for OUD and for predicting treatment response.

Human neuroimaging studies have provided valuable insight into the neural correlates of OUD (1–4). However, such investigations are challenged by the marked individual variability in polysubstance abuse and duration of use. In contrast, rodent models offer a controlled environment in which to study the mechanisms of chronic opiate effects on the brain. In the interest of identifying brain regions that are critically involved in drug reward, dependence, and withdrawal, expression of the immediate early gene *c-Fos* has been widely used in preclinical rodent models as a marker for neuronal activity. Induction of *c-Fos* occurs following both acute and chronic exposure to drugs of abuse and during withdrawal, and its expression is correlated with drug-induced behavioral changes including locomotor sensitization, conditioned place preference (CPP), and conditioned place aversion (5–7).

Four weeks of abstinence from chronic morphine exposure prior to conditioning has been shown to increase morphine CPP in rats, suggesting that rewarding properties of the drug are enhanced following protracted withdrawal (8). This enhanced preference is also associated with increased FOS expression in the cingulate cortex, nucleus accumbens (NAc), bed nucleus of the stria terminalis (BNST), and central and basolateral amygdala (CeA and BLA) (8). Induction of FOS protein expression in the NAc core and shell, dorsal striatum, ventral pallidum, lateral hypothalamus, and cortical regions following acute morphine has also been shown in rodent models (9), with the NAc and striatum displaying the most consistent activation across studies.

Analysis of FOS expression in rodent models has been critical for identifying individual brain regions associated with opioid exposure. However, OUD is a complex disease that will require a holistic rather than reductionist approach to fully appreciate its biological underpinnings. Studying the activity of individual regions in isolation ignores higher-order relationships between regions that form networks, in which individual brain regions may be represented as nodes, and their functional associations may be represented as edges (10, 11). Dynamics on these networks can be studied mathematically using tools from network control theory (12).

Significance

Persistent alterations to neural circuitry may help to explain why opiate abuse liability is higher among individuals with a history of chronic exposure. In this study, we employ a unique combination of computational approaches to understand how opiate-induced reorganization of network connectivity is supported by transcriptional and structural features of the brain. We identify a persistent reduction in FOS correlation network strength following opiate dependence and determine that correlated gene expression is predictive of opiate-induced changes in network connectivity. Further, we identify brain regions that influence the transition between opiate-naïve and opiate-dependent states. These findings establish a link between gene expression and changes in brain connectivity in response to opioids.

Author contributions: J.K.B. and J.A.B. designed research; J.K.B., K.D.M., and C.W. performed research; E.J.C., F.P., and D.S.B. contributed new reagents/analytic tools; J.K.B. analyzed data; and J.K.B. and J.A.B. wrote the paper.

The authors declare no competing interest.

This article is a PNAS Direct Submission. O.S. is a guest editor invited by the Editorial Board.

Data deposition: FOS expression data and all code used for the analyses are available at https://github.com/jkbrynildsen/opiateFOSconnectivity.

[1]To whom correspondence may be addressed. Email: blendy@pennmedicine.upenn.edu.

This article contains supporting information online at https://www.pnas.org/lookup/suppl/doi:10.1073/pnas.2003601117/-/DCSupplemental.

First published July 21, 2020.

The basic premise to be investigated in the current study is that chronic exposure to opioids causes changes in FOS correlation networks, which we define as interregional correlations in neuronal activation across subjects. We hypothesize that these changes occur in key areas of the brain that may predispose an individual to increased drug-seeking behavior. To this end, we apply a combination of computational approaches (graph theory and network control theory) to 1) define characteristics of FOS correlation networks associated with opioid dependence, 2) characterize gene expression patterns associated with changes in FOS correlation network connectivity induced by opioid dependence, and 3) identify brain regions that are most influential in the transition from an opiate-naïve to an opiate-dependent brain state (overview of design in Fig. 1). The analysis of complex networks with respect to OUD could shed light on the causes and mechanisms of the disease and provide compelling targets for therapeutic interventions.

Results

Acute Morphine Increases FOS Expression in a State-Dependent Manner. To test the hypothesis that dependence alters neuronal activity in response to morphine, we administered an acute, rewarding dose of morphine (10 mg/kg) to mice in three states: drug-naïve, 24 h after chronic exposure (at which time dependence has been established, as evidenced by increased somatic signs of withdrawal shown in *SI Appendix*, Fig. S1), and 4 wk after chronic exposure. FOS expression was quantified in each of these three treatment groups and in a saline-injected control group within 19 brain regions of interest. All FOS expression values were normalized to the mean FOS expression in saline-injected controls to compute fold change (13). Analysis of fold change in FOS expression by two-way ANOVA revealed significant main effects of brain region ($F_{18,570} = 19.52$, $P < 0.0001$) and treatment ($F_{3,570} = 104.0$, $P < 0.0001$) and a significant region × treatment interaction ($F_{54,570} = 4.493$, $P < 0.0001$) (Fig. 2).

We performed Bonferroni post hoc tests over all 19 families of six pairwise comparisons for each brain region and set the statistical threshold for a significant difference in FOS expression between any two treatment groups to $P < 0.05$. We observed state-dependent increases relative to saline controls within 12 brain regions: the dorsal anterior cingulate cortex (dACC), ventral anterior cingulate cortex (vACC), dorsal agranular insula (AId), claustrum (Cla), caudate putamen (CPu), NAc, BNST, BLA, CeA, lateral habenula (LHb), compact region of the substantia nigra (SNc), and ventral tegmental area (VTA). Mice in all morphine-treated groups showed elevated FOS expression in the dACC, Cla, CPu, NAc, BNST, and BLA relative to saline-treated controls. In the BLA, FOS expression was also significantly elevated at 24 h compared to in the naïve state. In the CPu, FOS expression was also significantly greater after 4 wk compared to in the naïve state. In the dACC, FOS expression was significantly greater in the naïve condition compared to 24 h, and in both the dACC and VTA, FOS expression was significantly elevated 4 wk after chronic exposure relative to all other conditions. FOS expression increased only in mice with prior chronic exposure in the AId (at 24 h), in the LHb and SNc (at 4 wk), and in the CeA (at 24 h and 4 wk). In the vACC, FOS expression increased only in the naïve and 4-wk groups, and the 4-wk group showed significantly higher expression than the 24-h group. FOS expression was not significantly elevated in the ventral agranular insula (AIv), ventral pallidum (VP), dentate gyrus (DG), medial habenula (MHb), paraventricular nucleus of the thalamus (PVT), periaqueductal gray (PAG), or reticular region of the substantia nigra (SNr) in any treatment group. Thus, neuronal activity in response to an acute dose of morphine is significantly different depending on brain state.

Chronic Opiate Exposure Alters Network Connectivity. After identifying region-specific effects of morphine dependence on FOS expression, we next sought to characterize network-level changes in interregional FOS correlation networks across brain regions. We generated FOS correlation networks based on pairwise interregional correlations in FOS expression across mice. Interregional Pearson's correlation coefficients were calculated based on fold change in FOS expression (relative to saline) in 19 brain regions (Fig. 3*A*). Each brain region is represented as a node in the network, and correlations in FOS expression are represented as edges which are weighted according to the strength of the correlation (Fig. 3*C*). A one-way ANOVA of Fisher's *z*-transformed positive Pearson's *r* values revealed a significant reduction in mean correlation strength 24 h after chronic exposure compared to in the drug-naïve state, and this reduction is maintained 4 wk after chronic exposure (Fig. 3*B*). These data indicate that opioid dependence induces a reduction in functional coupling between brain regions that persists across time, as reflected by the striking difference in connectivity between states (Fig. 3*C*). We observed the same results when using Spearman correlations instead of Pearson correlations (*SI Appendix*, Fig. S2).

A common objective of graph theory approaches to network analysis is to identify nodes that are relatively "central" within the network, which may suggest an important role in information flow between other nodes (14, 15). Here, we used two centrality measures to assess local connectivity within the global context of our networks: weighted degree and weighted betweenness centrality. Weighted degree refers to the sum of edges connected to a given node, weighted by their strength (16). Nodes with high degree are often referred to as network hubs and may strongly influence the network's function (14, 15). Betweenness centrality refers to the number of shortest paths between other nodes that a given node intersects (14). In the context of this work,

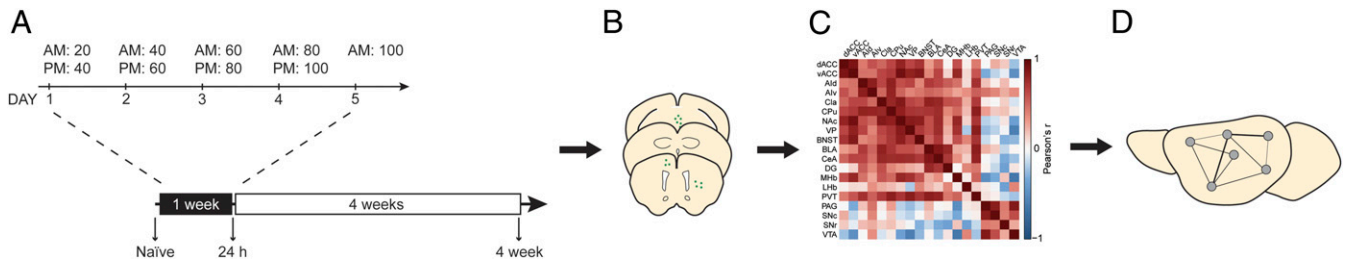

Fig. 1. Experimental schematic. (*A*) Three groups of mice were administered 10 mg/kg morphine in three states: drug-naïve, 24 h after chronic morphine, and 4 wk after chronic morphine. The chronic morphine exposure paradigm consisted of 5 d of repeated s.c. injections of escalating doses of morphine. Doses shown are in milligrams per kilogram. Control animals were given injections of saline instead of morphine. (*B*) Tissue was collected 90 min after the last injection, 30-μm sections were cut on a cryostat, and populations of neurons were quantified within 19 brain regions of interest. (*C*) Interregional correlation matrices were generated from FOS quantification data. (*D*) FOS correlation networks were used to formally represent interregional correlation matrices.

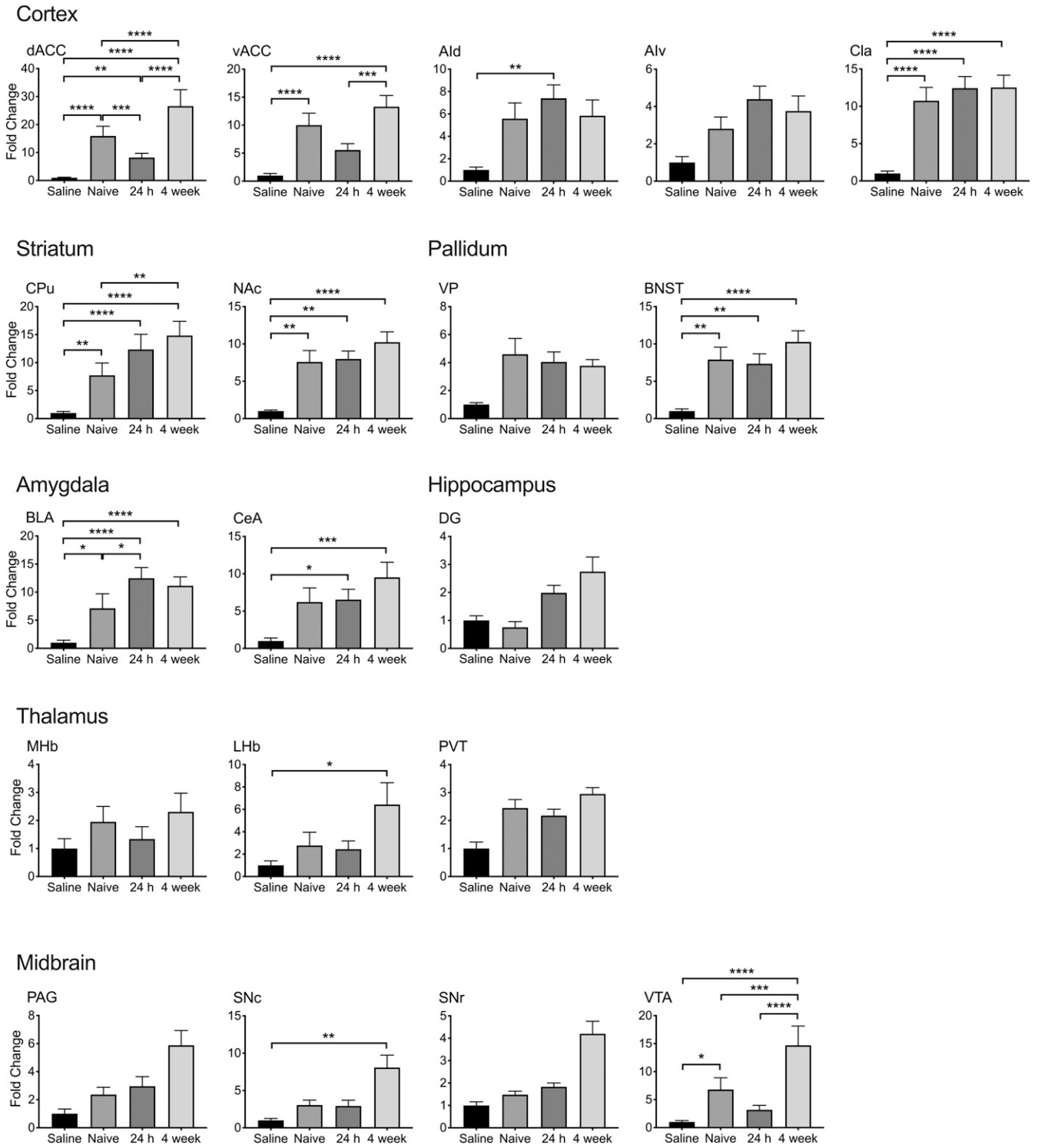

Fig. 2. Acute morphine increases FOS expression in a state-dependent manner. Fold change in FOS expression relative to saline group in 19 brain regions. Male C57BL/6 mice (n = 8 or 9 per group) were administered an injection of 10 mg/kg morphine after no prior drug exposure (naïve), 24 h after chronic exposure (24 h), or 4 wk after chronic exposure (4 wk), and tissue was collected 90 min later. The influence of treatment on fold change in FOS expression across brain regions was analyzed by two-way ANOVA. Bonferroni-corrected *P < 0.05, **P < 0.01, ***P < 0.001, ****P < 0.0001. Error bars represent SEM.

betweenness centrality reflects the extent to which one brain region acts as an intermediary between other brain regions.

Analysis by two-sample Kolmogorov–Smirnov test revealed that relative to the naïve state, networks significantly differed in distributions of weighted degree at 24 h (D_{36} = 0.6316, P = 0.0021) and 4 wk (D_{36} = 0.5263, P = 0.028) after chronic morphine exposure (Fig. 3*D*). There was no change in weighted degree distribution between 24 h and 4 wk (D_{36} = 0.3158, P = 0.92). To examine region-specific changes in weighted degree across conditions, we performed a two-way ANOVA and

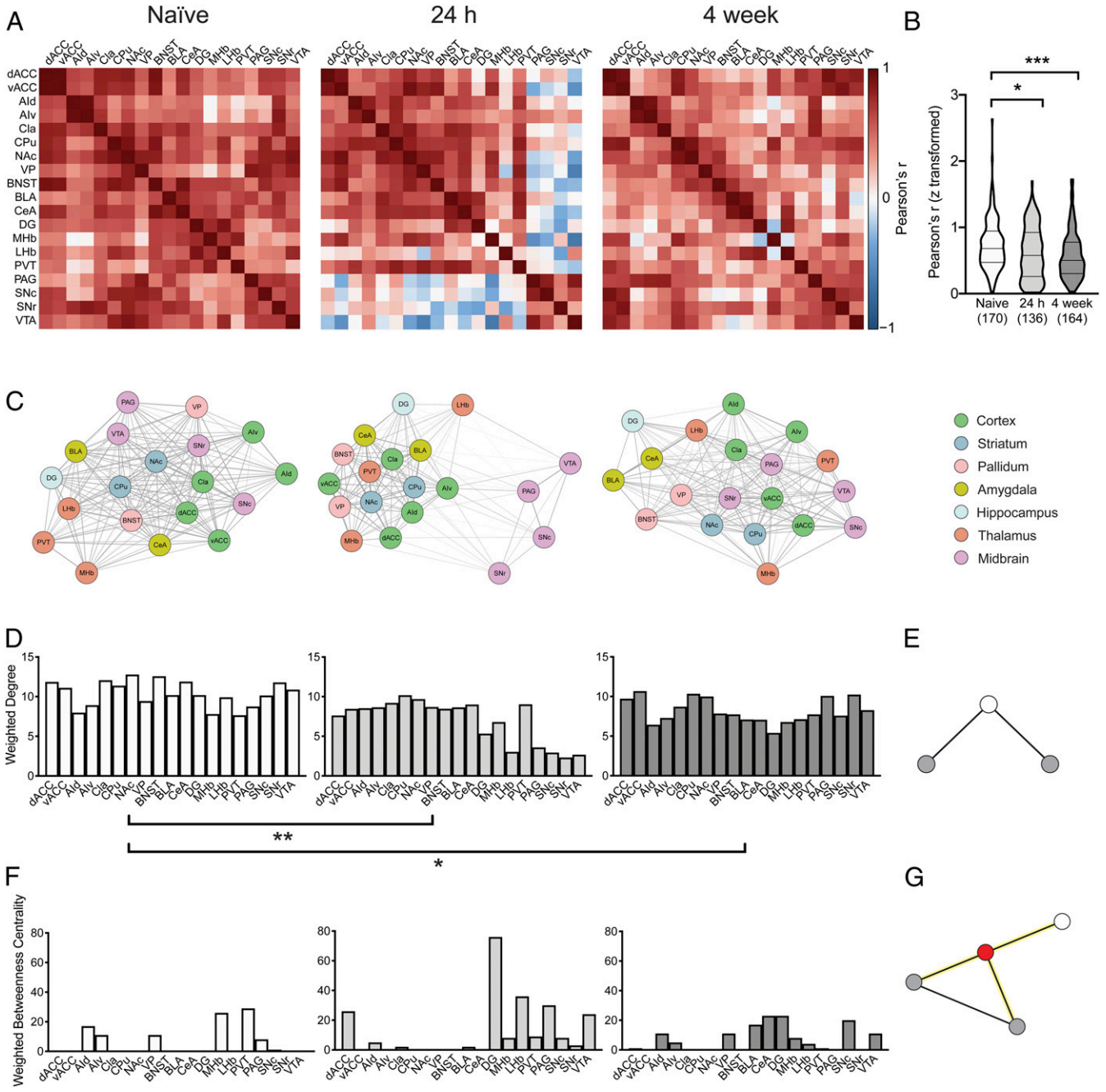

Fig. 3. Opioid dependence alters local features of FOS correlation network connectivity. (*A*) Interregional correlation matrices reflecting pairwise correlations in FOS expression between 19 brain regions of interest. (*B*) Distribution of Fisher's *z*-transformed positive Pearson's *r* values across states. (*C*) Graph representations of FOS correlation networks reflecting the correlation matrices. Nodes represent brain regions, and edges represent positive pairwise correlations in FOS expression, weighted according to the strength of the correlation. Nodes are colored to reflect their anatomical class. (*D*) Weighted degree in each state. (*E*) Illustration of degree. Each of the gray nodes has a degree of 1, while the white node has a degree of 2. (*F*) Weighted betweenness centrality in each state. (*G*) Illustration of betweenness centrality. The red node falls on the shortest paths (highlighted) between each of the gray nodes and the white node. Distributions of weighted degree and betweenness centrality were compared via two-sided Kolmogorov–Smirnov test. Bonferroni-corrected $^{*}P < 0.05$, $^{**}P < 0.01$, $^{***}P < 0.001$.

identified significant main effects of region ($F_{5,39} = 7.743$, $P < 0.0001$) and treatment ($F_{2,39} = 23.95$, $P < 0.0001$) and a significant region × treatment interaction ($F_{10,39} = 4.161$, $P = 0.0006$). In regions of the midbrain, weighted degree was significantly reduced at 24 h after chronic exposure compared to in the naïve and protracted withdrawal states (Bonferroni-corrected $P < 0.0001$). Nonsignificant reductions in weighted degree were observed across all other region groups in the 24-h and 4-wk states relative to the naïve state (*SI Appendix*, Fig. S3*A*). Distributions of weighted betweenness centrality did not differ across states ($D_{36} \leq 0.3158$, $P \geq 0.90$) (Fig. 3*E*), and region-specific analysis by two-way ANOVA revealed a significant main effect of region ($F_{5,39} = 2.523$, $P = 0.0451$) but no effect of treatment ($F_{2,39} = 0.6490$, $P = 0.5281$) and no region × treatment interaction ($F_{10,39} = 1.144$, $P = 0.3562$) (*SI Appendix*, Fig. S3*B*). Taken together, these findings suggest that opioid dependence alters the

functional architecture of the brain by modulating the strength of connections between pairs of regions, particularly within the midbrain, but not by altering the tendency for brain regions to mediate connections between other regions.

Basal Gene Expression Patterns Predict Change in FOS Correlation Networks following Opioid Dependence. We next sought to identify a transcriptional basis for opiate-induced changes in FOS correlation networks. We used transcriptomic data recently released by the Allen Institute, which allows for the spatial resolution of gene expression across brain regions. This dataset was used to examine correlated gene expression patterns across 19,616 genes within our 19 brain regions of interest. We defined gene coexpression as spatially-corrected pairwise correlations in expression across all genes between every pair of brain regions. We then performed a linear regression of mean gene coexpression per brain region with change in weighted degree from the drug-naïve to the 24-h state. We hypothesized that basal gene expression may play a role in how certain brain regions are functionally connected. Of interest, we identified a significant, positive linear relationship between basal gene coexpression and changes in FOS correlation networks that result following chronic opioid exposure (Fig. 4*A*). Specifically, we observed stronger gene coexpression among pairs of brain regions that show increased connection strength after opioid exposure, compared to those that show decreased connection strength. Thus, basal gene coexpression patterns are predictive of changes in FOS correlation networks following chronic opioid exposure.

To identify specific genes that contribute significantly to the higher coexpression among pairs of regions that show increased connection strength compared with those that show decreased connection strength (Fig. 4*B*) we calculated a gene coexpression contribution (GCC) score for each gene (17), which yields a *t*-statistic score and *P* value for each gene. After applying a false discovery rate correction ($q < 0.05$) for multiple comparisons across the 19,616 tests, we identified 2,775 genes that significantly contribute to higher gene coexpression among brain region pairs that show increased connectivity compared to brain region pairs that show decreased connectivity following opioid dependence. In order to appreciate the biological significance of these genes, we used Ingenuity Pathway Analysis software to functionally annotate genes that contribute to stronger transcriptional coupling between regions that show increased connectivity following opioid dependence. Among the most significantly associated pathways were Synaptic Long Term Potentiation, Synaptogenesis Signaling Pathway, Integrin Signaling, and Reelin Signaling in Neurons (Table 1). These findings are in line with the notion that drugs of abuse alter synaptic transmission, which is reflected by changes in FOS correlation networks.

Network Control. Drug dependence is understood to coincide with a change in the state of the brain. A major challenge in the treatment of substance use disorders is determining how to restore the brain to its former state (18). Reaching this goal will require an understanding not only of how neural circuitry is altered by drug dependence but also of the molecular and physiological mechanisms that drive persistent circuitry alterations in the brain.

In the interest of identifying potential therapeutic targets for OUD, we sought to identify brain regions that drive network-level changes in neuronal activity. To this end, we employed a network control theory approach. Network control is an emerging approach in systems engineering with marked utility in neuroscience (19–24). Control in the brain may be exerted internally (for example, via cognitive control) or externally (for example, via stimulation). In recent years, control theory approaches have been applied to examine cognitively relevant brain-state transitions observed in human functional magnetic resonance imaging data (20, 25–27).

Here, we used network control theory to explore how OUD-dependent changes in FOS expression may be mediated by the topology of axonal connections in the brain. The approach posits that transitions between states are constrained by the energy required to transmute one state into another, allowing activity to spread solely through known structural interregional links. Specifically, we computed the minimum whole-brain input energy required to transition between brain activity patterns associated with different opioid-dependence states. Brain activity is represented by fold change in FOS expression vectors and the brain network is defined by interregional axonal connection strength obtained from the Allen Mouse Brain Atlas (28). In principle, this approach measures the ease with which the brain can transition from a drug-naïve to a drug-dependent activity state, and from a drug-dependent to a protracted withdrawal activity state (Fig. 5*B*), given the constraints imposed by the topology of axonal connections between the measured regions. Our model does not distinguish the drivers of such transitions, which in this case are likely a combination of internal neuronal dynamics and external inputs (i.e., opiate exposure).

For each state transition, the minimum control energy was first calculated under full control (meaning external input can be delivered to all regions) and then recalculated following suppression of each region (external input can be delivered to all regions except the suppressed region). This analysis determines the increase in minimum control energy induced by the removal

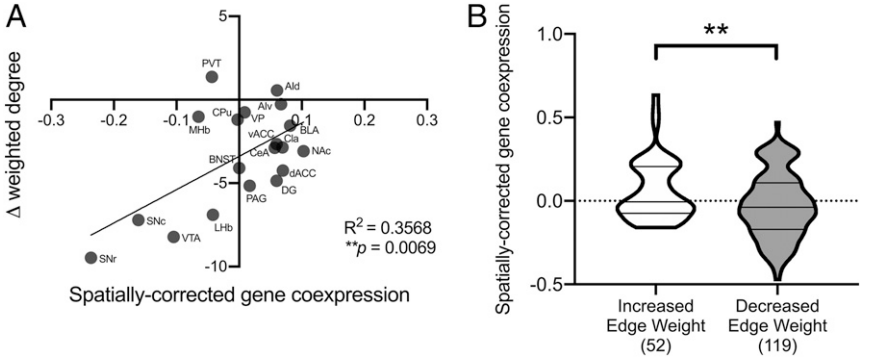

Fig. 4. Gene coexpression patterns predict changes in network connectivity strength induced by opiate dependence. (*A*) Linear regression between gene coexpression and the change in FOS correlation networks from an opiate-naïve state to 24 h after withdrawal from chronic exposure. (*B*) Distribution of edges showing increased weight following opiate dependence, compared to edges showing decreased weight following opiate dependence. $^{**}P < 0.01$.

Table 1. Genes implicated in synaptic plasticity are associated with changes to FOS correlation networks following opioid dependence

Pathway	Ratio	*P* value
Fcγ Receptor-mediated Phagocytosis in Macrophages and Monocytes	0.266	1.15E-06
Neuropathic Pain Signaling In Dorsal Horn Neurons	0.257	1.38E-06
Endocannabinoid Neuronal Synapse Pathway	0.242	6.03E-07
Synaptic Long Term Potentiation	0.240	7.24E-07
Reelin Signaling in Neurons	0.233	2.24E-06
CREB Signaling in Neurons	0.203	1.23E-06
Integrin Signaling	0.197	2.69E-06
Synaptogenesis Signaling Pathway	0.192	5.62E-08
Molecular Mechanisms of Cancer	0.187	7.76E-09

Pathways most highly significantly associated with increased gene coexpression among pairs of brain regions showing increased connectivity following opioid dependence compared to pairs of brain regions showing decreased connectivity. Pathways are ranked in order of the proportion of overlap between significantly associated genes and total genes within the pathway (Ratio).

of each brain region which, in essence, quantifies the relative influence of each brain region in the transition from one state to another. Relative to all other regions in the network, we identified nine brain regions that influence minimum control energy for the transition from a naïve state to 24-h "dependent" state: the vACC, CPu, NAc, VP, BNST, CeA, DG, PAG, and SNr (Table 2). These same regions, with the addition of the LHb and VTA, influence minimum control energy for the transition from the 24-h "dependent" state to the 4-wk protracted withdrawal state. The CPu, DG, and PAG stand out in the transition from naïve to dependent state, while the PAG and SNr most strongly influence minimum control energy for the transition from the 24-h to 4-wk states (Fig. 5*B*). In contrast, cortical and thalamic regions do not appear to significantly impact either state transition. Together, these findings indicate that regions of the hippocampus, striatum, and midbrain may be topologically positioned to facilitate easy transitions between activity patterns associated with different states of opioid dependence.

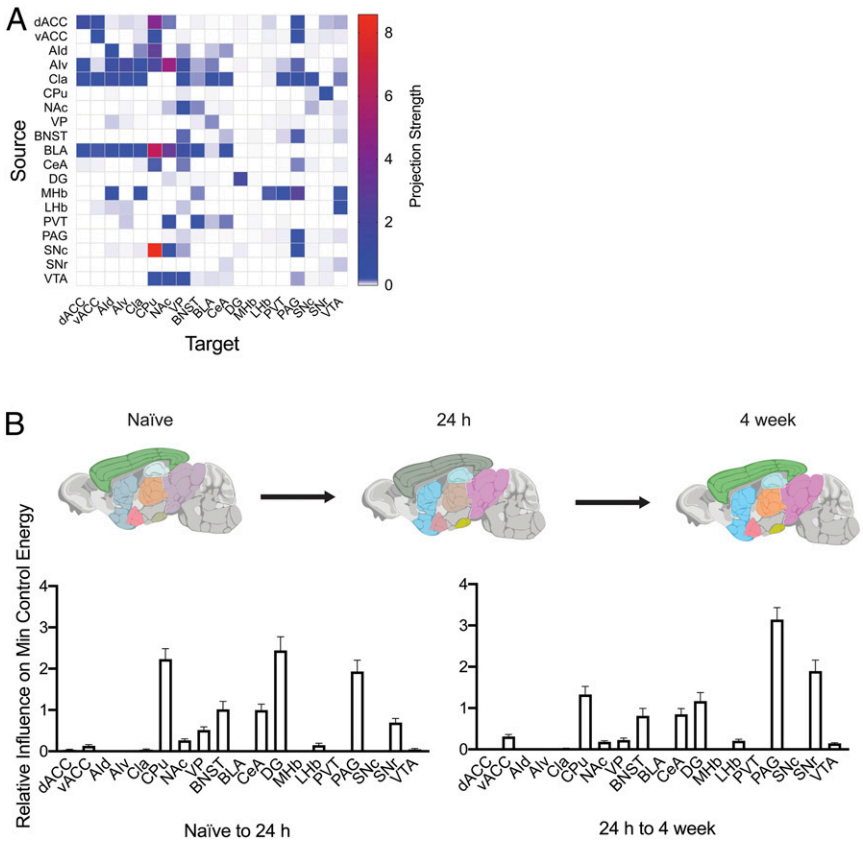

Fig. 5. Region-specific effects on control energy to drive the brain from a drug-naïve to a drug-dependent state. (*A*) Structural connectivity matrix representing quantitative projection strength values from the Allen Mouse Brain Connectivity Atlas. (*B*) Increase in minimum control energy to drive the brain between states. Brain images represent FOS expression levels in each state, where colors represent anatomical groups and opacity represents the expression level (more opaque indicates higher expression). Bar graphs depict the mean increase in minimum control energy following suppression of each region in the transition from the naïve to the 24-h state and from the 24-h to the 4-wk state. Error bars represent SEM.

Table 2. Relative influence of individual brain regions on minimum control energy for opiate-induced state transitions

Region	*P* value	
	Naïve to 24 h	24 h to 4 wk
dACC	1	0.9817
vACC	1.29E-09	1.51E-15
AId	1	0.9902
AIv	0.9191	0.9817
Cla	1	1
CPu	2.31E-42	6.99E-32
NAc	1.45E-18	2.02E-15
VP	3.06E-25	2.02E-15
BNST	1.82E-28	1.46E-22
BLA	1	0.9902
CeA	1.32E-28	6.99E-32
DG	2.31E-42	6.99E-32
MHb	1	1
LHb	0.9999	2.02E-15
PVT	1	1
PAG	1.75E-35	2.47E-46
SNc	1	1
SNr	1.82E-28	7.79E-39
VTA	1	2.02E-15

P values associated with the relative influence of each brain region on the minimum control energy for the transition from the naïve to 24-h state and from the 24-h to 4-wk state, as inferred from the increase in minimum control energy induced by removal of each region from the control set. A single *P* value for each region was obtained by using Fisher's method to combine *P* values from one-sided Welch's *t* tests between each region and all other regions in the network.

Discussion

Here we sought to determine the impact of opiate dependence on FOS correlation network connectivity, to identify gene coexpression patterns that predict opiate-induced changes in FOS correlation networks, and to determine the relative contributions of key brain regions to the minimum control energy required to drive the brain from one functional state of dependence to another. To this end, we describe network analyses of interregional FOS expression in 19 brain regions in three states: opiate-naïve, 24 h after chronic opiate exposure, and 4 wk after chronic opiate exposure. Morphine is known to induce FOS expression throughout the brain; however, our data demonstrate that the FOS response varies in a state-dependent manner. Pairwise interregional correlations in FOS expression were used to generate weighted networks, which reflect a significant reduction in mean positive correlation strength following chronic morphine exposure, suggesting that the strength of FOS correlation networks between brain regions is state-dependent. Finally, we show that axonal connectivity between regions of the striatum, midbrain, and hippocampus is critical for low-energy state transitions between functional states of opioid dependence. These data support the notion that repeated exposure to addictive drugs induces reorganization of neural circuitry that may underlie behaviors characteristic of addiction.

To capture the relationship between basal transcriptional coupling patterns and opiate-induced changes in FOS correlation networks, we examined gene coexpression patterns between all brain regions included in our study. Pathway analysis revealed that genes implicated in synaptic long-term potentiation, synaptogenesis, and reelin signaling were among the most significantly associated with increased FOS correlation networks following chronic opiate exposure (Table 1). Many drugs of abuse, including opioids, induce synaptic plasticity, suggesting that this type of neuroadaptation may be a common mechanism underlying the development of substance use disorders (29–31). Moreover, polymorphisms in genes associated with synaptic plasticity have been associated with vulnerability to drug addiction (32, 33). Our data indicate that coordinated expression of genes implicated in synaptic plasticity may predispose pairs of brain regions to increased FOS correlation networks induced by opiate dependence.

While graph theory metrics offer valuable approaches for characterizing connectivity properties, network control theory posits a mechanism for how interregional interactions give rise to state-dependent neural activity (19). Network control theory explains how a network may be driven to a particular activity state by modulating external inputs (19, 20). Here, we calculated the minimum input energy required to transition between brain activity patterns associated with drug-naïve and drug-dependent states. In the context of our work, opiate exposure is a major known external input, and we identify brain regions whose structural connectivity strongly influence the magnitude of input required to drive the brain into opiate-dependent activity states.

With respect to drug addiction, the brain and associated cellular and molecular mechanisms may adapt to chronic drug exposure differently depending on the individual. Indeed, epidemiological and clinical research has shown that most individuals who use drugs do not develop dependence. While environmental stressors and genetic factors can contribute to an individual's propensity to addiction, addiction vulnerability may also depend on the ease of transition from a drug-naïve to a drug-dependent brain state. In order to assess the relative influence of each brain region on the minimum energy associated with each transition, we calculated the change in minimum control energy following suppression of each brain region in the network (25). This simulated suppression of activity may be conceptualized as inhibitory neuromodulation, such as that induced by optogenetic inhibition (34), or noninvasively by transcranial magnetic stimulation (20, 35, 36). Clinically, such inhibitory neuromodulation could arise from aberrant brain pathology that involves region damage or loss.

In the naïve state, morphine increased FOS expression in eight regions of interest: the dACC, vACC, Cla, CPu, NAc, BNST, BLA, and VTA. These regions represent components of the mesocortical and mesolimbic dopamine systems which are implicated in drug incentive salience and acute reinforcing effects, respectively (37). In particular, dopaminergic neurons that project from the VTA to the NAc and cortical regions play an important role in acute, rewarding effects of morphine and other drugs of abuse (38–40). Several of these regions (the vACC, CPu, NAc, and BNST) were among those found to significantly influence minimum control energy for the transition from the naïve state to the 24-h "dependent" state. Of interest, regions that showed significant differences in FOS expression between the naïve and 24-h states (the dACC and BLA) were not among those found to significantly influence control energy for the state transition.

The dorsal striatum (CPu), DG, and PAG regions were found to most strongly influence the minimum control energy required to transition from an opiate-naïve to an opiate-dependent state (naïve to 24 h). The observed state transitions occur as a result of external inputs that include opiate exposure, and thus, in theory, more of that input would be required if a particularly influential region was suppressed. This suggests that inhibiting a region that strongly influences minimum control energy would prevent opiate exposure from leading to the dependent activity state.

Among the regions included in our analysis, the CPu also had the highest weighted degree in the 24-h state. This finding is consistent with previous work demonstrating that weighted degree is highly correlated with average controllability; specifically, suppression of regions with stronger connectivity increases minimum control energy more than suppression of regions with weaker connections (20). The CPu or dorsal striatum, in addition

to having a role in motor function, is involved in a number of important functions including cognition, decision making, motivation, and reward perception (41–43). The location of the CPu in the structural network suggests that it also has an important role in the transition of the brain from a naïve state to an opioid-dependent state and, by extension, the behaviors associated with brain activity patterns in those states as well.

The DG region of the hippocampus is critical for the acquisition of new memories and as such plays a critical role in the storage of information relevant to drug cues and environmental stimuli associated with drug-taking behavior. Many addictive drugs, particularly after chronic administration, have been shown to promote synaptic plasticity in this region (44, 45). Further, our gene coexpression analysis identified Synaptic Long Term Potentiation and Synaptogenesis Signaling as two of the top pathways associated with stronger transcriptional coupling between regions with increased connectivity following opioid dependence. Thus, it is not surprising that the DG was identified as a prominent brain region influencing the transitions in brain state following opiate exposure.

The PAG is primarily associated with analgesia and tolerance to opioids. Opioid-sensitive neurons in the PAG have been shown to be hyperexcited during opioid withdrawal (46) and the PAG receives input from both cortical and midbrain regions. Thus, the PAG is well-positioned for coordinating functional transitions between brain states associated with dependence and withdrawal. While these three brain regions were not the only ones identified that influence control energy for state transitions following opioid exposure and withdrawal, they are functionally plausible as control regions to help mediate transitions in brain state following opiate exposure.

Methodological Considerations. We note several methodological considerations pertinent to this work. First, the brain regions included in this analysis were chosen based on their known involvement in opiate reward, dependence, and withdrawal and were intended to be representative. To more completely characterize whole-brain connectivity under various drug states, future studies could include additional brain regions to promote a better understanding of how opioid dependence may alter associations between brain regions that are directly implicated in drug dependence and those that are not. Second, the network control approach that we used here assumes that activity flows along structural paths alone and follows linear dynamics (47). An extension to nonlinear dynamics constitutes a natural direction for future work.

Conclusion

Here, we report findings from a network analysis of FOS expression in 19 brain regions following acute morphine exposure in animals that were drug-naïve, drug-dependent, or had undergone 4 wk of withdrawal from chronic morphine exposure. We have combined the descriptive power of graph theory with the explanatory power of network control theory to identify opiate-induced alterations to FOS correlation networks. This innovative approach allows us to understand not only what changes occur but how they occur in the context of opioid dependence. Approaches like this can eventually provide a theoretical foundation upon which to understand the effects of interventions on the brain at a systems level.

Methods

Animals. Eight-week-old male C57BL/6 mice ($n = 34$ mice total; eight or nine per treatment group) obtained from Taconic Biosciences were used in the experiments. Mice were maintained on a standard light cycle (lights on between 0600 and 1800 h), with ad libitum access to food and water. All experimental procedures were approved by the University of Pennsylvania's Animal Care and Use Committee.

Drug Exposure. Morphine sulfate was obtained from the NIDA Drug Supply and dissolved in 0.9% saline. Dependence was induced by repeated, subcutaneous (s.c.) injections of escalating doses of morphine (Fig. 1 and *SI Appendix*, Fig. S1). Prior to tissue collection, an acute dose of 10 mg/kg s.c. morphine was given to induce FOS expression in each group of mice.

FOS Immunohistochemistry. Mice were deeply anesthetized with sodium pentobarbital (50 mg/kg intraperitoneally) 90 min after receiving an injection of 10 mg/kg morphine (s.c.) and were perfused with 20 to 30 mL ice-cold 0.01M phosphate-buffered saline (PBS), followed by 40 to 50 mL ice-cold 4% paraformaldehyde (PFA). Brains were postfixed overnight in 4% PFA and cryoprotected in 30% sucrose at 4 °C. Brains were then frozen at −20 °C and 30 μm sections were cut on a cryostat.

After slide mounting, sections were washed four times for 10 min in 0.01M PBS, blocked for 1 h in 0.01M PBS containing 5% normal goat serum and 0.3% Triton X-100, and incubated overnight at room temperature in rabbit anti-cFOS primary antibody (1:300 dilution, 2250S; Cell Signaling). Sections were then washed four times for 10 min in 0.01M PBS, incubated for 1 h in goat anti-rabbit Alexa Fluor 488 secondary antibody (1:1,000 dilution), and again washed four times for 10 min in 0.01M PBS. Prior to imaging, slides were coverslipped with DAPI Fluoromount.

Image Acquisition and Quantification. The following regions were imaged and included in the analysis: dACC and vACC, AId and AIv, Cla, CPu, NAc, VP, BNST, BLA, CeA, DG, MHb and LHb, PVT, PAG, SNc and SNr, and VTA. Images were acquired as 1-μm z-stacks at 20× magnification on a Keyence BZ-X800 fluorescence microscope and stitched to capture entire brain regions within the coronal plane. The maximum projection images were used to quantify FOS expression. Regions of interest were defined according to the Allen Mouse Brain Atlas (28), and FOS-expressing cells within each region were quantified using Fiji software (48). FOS-positive cells per square millimeter were counted and summed across both hemispheres by two experimenters blinded to treatment condition and averaged across three sections per brain region. In order to account for FOS expression induced by handling and injection stress, quantifications of FOS expression for each mouse were normalized to the mean FOS expression of saline-injected controls to compute fold change (Fig. 2). Two-way ANOVA of fold change in FOS expression was performed using GraphPad Prism software, and P values were Bonferroni-corrected for multiple comparisons.

Network Construction. Undirected, weighted networks were constructed in which brain regions of interest served as nodes and positive pairwise Pearson's correlations in fold change in FOS expression across animals served as edges between nodes (49). A one-way ANOVA was used to compare Fisher z-transformed correlation coefficients between states. Correlation matrices were generated using the package corrplot (50), represented as graphs, and both visualized and analyzed using the package igraph (51) within R (52). The two-dimensional projections of networks for visualization purposes were constructed using the Fruchterman–Reingold algorithm (53).

In the context of our work, regions of the network are deemed to be "connected" when there exist statistical dependencies in interregional patterns of neuronal activity across animals. Thus, differences in interregional correlation values between states reflect increases or decreases in the similarity of interregional neuronal activity patterns induced by chronic opiate exposure. Regions that display positive interregional correlations in neuronal activity are understood to be functionally associated, and changes in correlation values may reflect altered communication between brain regions.

Local Characteristics of Network Connectivity. To characterize FOS correlation network connectivity, we computed the distributions of weighted degree and weighted betweenness centrality for each network. Weighted degree gives the number of edges connected to a node, weighted according to strength; in this case, the weight reflected the strength of the positive pairwise correlation. The weighted degree is defined as

$$s_i = \sum_{j=1}^{N} a_{ij} w_{ij},$$

where a_{ij} represents the connection between nodes i and j, w_{ij} represents the weight of the connection between nodes i and j, and N is the set of all nodes in the network (16).

The weighted betweenness centrality gives the number of shortest paths in a weighted network on which a given node lies. The weighted betweenness of each node i is defined as

$$b_i^w = \sum_{h,\ j\in N, h\neq j, h\neq i, j\neq i} \frac{\sigma_{hj}^w(i)}{\sigma_{hj}^w},$$

where σ_{hj}^w is the number of weighted shortest paths between node h and node j and $\sigma_{hj}^w(i)$ is the number of weighted shortest paths between node h and node j that pass through node i (54). Weighted degree and weighted betweenness centrality were computed using the package igraph within R, and two-sample Kolmogorov–Smirnov tests were used to compare the distributions of degree and betweenness centrality between each pair of states. The resultant P values were Bonferroni-corrected for multiple comparisons.

Gene Expression Analysis. Regional gene expression data were obtained from the Allen Mouse Brain Atlas microarray data available at download.alleninstitute.org/informatics-archive/october-2014/mouse_expression/mouse_expression_data_sets.csv. For each available experiment, we first normalized the expression intensity of each gene across regions using a sigmoid function (17) in order to account for arbitrary differences in baseline signal across experiments. This process yields an $N \times 1$ vector of gene expression on a scale of 0 to 1 for each experiment for each gene, where N is the number of brain regions (here, the 19 brain regions assayed for FOS expression). Next, for each gene, we averaged expression vectors across all available probes and experiments, yielding an $N \times 19{,}616$ matrix of gene expression values for each region.

We assessed gene coexpression patterns by calculating pairwise interregional Pearson's correlations in expression across 19,616 genes. We adjusted for spatial correlations in the data by fitting an exponential decay curve $r_g(d_{ij}) = 1.2201e(-0.6008\, d_{ij}) - 0.1491$ (*SI Appendix*, Fig. S4). To understand the relationship between gene coexpression and opiate-induced change in connectivity strength, we performed a linear regression of mean gene coexpression with change in weighted degree from the opiate-naïve to opiate-dependent state for each brain region. We then used a two-sided Welch's t test to compare gene coexpression between all pairs of brain regions that show increased connectivity strength and all pairs of brain regions that show decreased connectivity strength following opiate dependence. In order to identify the specific genes that contribute to higher gene coexpression between brain region pairs that show increased FOS correlation networks after opioid dependence, we computed a GCC score for each gene, which is defined as

$$GCC_{ij}^{(a)} = \tilde{g}_i^{(a)}\tilde{g}_j^{(a)} - r_g(d_{ij}),$$

where $\tilde{g}_i^{(a)}\tilde{g}_j^{(a)}$ is the product of z-scored, normalized gene expression values for gene a in brain regions i and j (17).

One-sided Welch's t tests were used to identify genes that significantly contribute to the observed higher gene coexpression levels among increased functional associations compared to decreased functional associations. To relate significantly associated genes to functional pathways, we then performed gene function analysis using Ingenuity Pathway Analysis (Version 01-14; QIAGEN). Ingenuity Pathway Analysis uses a Fisher's Exact Test to identify canonical pathways that are significantly associated with the genes of interest relative to the entire Ingenuity Pathway Analysis knowledge base.

Network Control. To understand how the brain is driven from an opiate-naïve to an opiate-dependent state, taking into consideration the structural connectivity of its component regions, we used a network control theory approach. Network control theory explains how to manipulate the state of a system of interconnected units (12, 55, 56). Given an understanding of the connections between elements in a system and the dynamics or activity of those elements, we can use network control theory to make predictions about the behavior of the system (19).

The simplified mathematical model that we used to describe the brain's dynamics when it is driven along a particular trajectory by injecting control signal or input is defined as

$$\dot{x} = Ax(t) + B_\kappa u_\kappa(t),$$

where $x(t)$ is an $N \times 1$ vector representing the state of the brain; in this case, each state is the fold change in FOS expression across $N = 19$ brain regions. The matrix A is an $N \times N$ adjacency matrix representing the relationships between brain regions; in the context of this work, it represents the density of axonal projections between each pair of regions (28). When all brain regions are controlled, B_κ is an $N \times N$ identity matrix with ones along the diagonal and zeros elsewhere. The variable $u_\kappa(t)$ is an $N \times 1$ vector reflecting the amount of control input into each of the N control regions at each time point t.

We computed the minimum control energy to transition between opiate-naïve and opiate-dependent brain states and used these values to determine the relative influence of each brain region on the state transition. The minimum control energy is the minimum energy of a control input to drive the brain from an initial state $x(0) = x_0$ to a target state $x(T) = x_T$ over time horizon T. To compute minimum control energy, the activity level (FOS expression) for each brain region in each state is specified, as is the control set B_κ. In order to compute the change in minimum control energy induced by removing brain region i from the control set, the i-th diagonal element in B_κ is replaced with a zero, and control energy in the full control condition is subtracted from the resulting control energy. In our study, minimum control energy was computed with a time horizon of 1 (27). Of note, we found that varying the time horizon did not alter the distribution of the results (*SI Appendix*, Fig. S5).

Minimum control energy was computed using MATLAB software. Structural connectivity data for regions corresponding to those included in the FOS correlation networks analysis were obtained from the Allen Mouse Brain Connectivity Atlas (28). Structural connectivity data were obtained from adult male C57BL/6 mice and represent the density of axonal projections mapped from each tracer-injected source node to its ipsilateral target node. Functional data under each state were represented by fold change in FOS expression for each brain region.

In order to statistically compare the relative influence of each brain region in the network on the minimum control energy necessary for each state transition, we computed the minimum control energy between every possible pair of FOS expression vectors in each state (e.g., given $n = 8$ mice in the naïve group and $n = 9$ mice in the 24-h group, 72 vector pairs are possible) after suppression of each brain region, as described above. One-sided Welch's t tests were used to identify brain regions that significantly influence the minimum control energy for each state transition relative to other brain regions. All P values were Bonferroni-corrected for multiple comparisons and were combined using Fisher's method to obtain a single P value for each region.

Data Availability. FOS expression data and all code used for the analyses are available at https://github.com/jkbrynildsen/opiateFOSconnectivity. Structural connectivity data and interregional distance data are available from the Allen Institute (28). Regional gene expression microarray data from the Allen Mouse Brain Atlas are available at download.alleninstitute.org/informatics-archive/october-2014/mouse_expression/mouse_expression_data_sets.csv.

ACKNOWLEDGMENTS. We thank Andrei Georgescu for brain illustrations shown in Fig. 5. This work was supported by National Institute on Drug Abuse Grants R01 DA041180 (J.A.B.) and T32 DA028874 (J.K.B.), NSF Grant BCS-1631550 (D.S.B.), and Army Research Office Grant W911NF-18-1-0244 (D.S.B.). The views and conclusions contained in this document are those of the authors and should not be interpreted as representing the official policies, either expressed or implied, of the Army Research Office or the US Government. The US Government is authorized to reproduce and distribute reprints for Government purposes notwithstanding any copyright notation herein.

1. H. Moningka *et al*., Can neuroimaging help combat the opioid epidemic? A systematic review of clinical and pharmacological challenge fMRI studies with recommendations for future research. *Neuropsychopharmacology* **44**, 259–273 (2019).
2. J. L. Stewart, A. C. May, R. L. Aupperle, J. Bodurka, Forging neuroimaging targets for recovery in opioid use disorder. *Front. Psychiatry* **10**, 117 (2019).
3. H. F.-H. Ieong, Z. Yuan, Resting-state neuroimaging and neuropsychological findings in opioid use disorder during abstinence: A review. *Front. Hum. Neurosci.* **11**, 169 (2017).
4. E. A. Cabrera *et al*., Neuroimaging the effectiveness of substance use disorder treatments. *J. Neuroimmune Pharmacol.* **11**, 408–433 (2016).
5. B. T. Hope, D. E. Simmons, T. B. Mitchell, J. D. Kreuter, B. J. Mattson, Cocaine-induced locomotor activity and Fos expression in nucleus accumbens are sensitized for 6 months after repeated cocaine administration outside the home cage. *Eur. J. Neurosci.* **24**, 867–875 (2006).
6. M. M. Pascual, V. Pastor, R. O. Bernabeu, Nicotine-conditioned place preference induced CREB phosphorylation and Fos expression in the adult rat brain. *Psychopharmacology (Berl.)* **207**, 57–71 (2009).
7. B. K. Tolliver, M. W. Sganga, F. R. Sharp, Suppression of c-fos induction in the nucleus accumbens prevents acquisition but not expression of morphine-conditioned place preference. *Eur. J. Neurosci.* **12**, 3399–3406 (2000).

8. G. C. Harris, G. Aston-Jones, Enhanced morphine preference following prolonged abstinence: Association with increased Fos expression in the extended amygdala. *Neuropsychopharmacology* **28**, 292–299 (2003).
9. B. Ziółkowska, M. Korostyński, M. Piechota, J. Kubik, R. Przewłocki, Effects of morphine on immediate-early gene expression in the striatum of C57BL/6J and DBA/2J mice. *Pharmacol. Rep.* **64**, 1091–1104 (2012).
10. D. S. Bassett, O. Sporns, Network neuroscience. *Nat. Neurosci.* **20**, 353–364 (2017).
11. D. S. Bassett, P. Zurn, J. I. Gold, On the nature and use of models in network neuroscience. *Nat. Rev. Neurosci.* **19**, 566–578 (2018).
12. Y.-Y. Liu, J.-J. Slotine, A.-L. Barabási, Controllability of complex networks. *Nature* **473**, 167–173 (2011).
13. J. K. Brynildsen *et al*, FOS expression data and code associated with "Gene coexpression patterns predict opiate-induced brain state transitions." GitHub. https://github.com/jkbrynildsen/opiateFOSconnectivity. Deposited 18 June 2020.
14. L. C. Freeman, Centrality in social networks: Conceptual clarification. *Soc. Networks* **1**, 215–239 (1978).
15. T. Opsahl, F. Agneessens, J. Skvoretz, Node centrality in weighted networks. *Soc. Networks* **32**, 245–251 (2010).
16. A. Barrat, M. Barthélemy, R. Pastor-Satorras, A. Vespignani, The architecture of complex weighted networks. *Proc. Natl. Acad. Sci. U.S.A.* **101**, 3747–3752 (2004).
17. B. D. Fulcher, A. Fornito, A transcriptional signature of hub connectivity in the mouse connectome. *Proc. Natl. Acad. Sci. U.S.A.* **113**, 1435–1440 (2016).
18. D. Goldman, C. S. Barr, Restoring the addicted brain. *N. Engl. J. Med.* **347**, 843–845 (2002).
19. S. Gu *et al*., Controllability of structural brain networks. *Nat. Commun.* **6**, 8414 (2015).
20. R. F. Betzel, S. Gu, J. D. Medaglia, F. Pasqualetti, D. S. Bassett, Optimally controlling the human connectome: The role of network topology. *Sci. Rep.* **6**, 30770 (2016).
21. S. F. Muldoon *et al*., Stimulation-based control of dynamic brain networks. *PLOS Comput. Biol.* **12**, e1005076 (2016).
22. E. Tang *et al*., Developmental increases in white matter network controllability support a growing diversity of brain dynamics. *Nat. Commun.* **8**, 1252 (2017).
23. J. Stiso *et al*., White matter network architecture guides direct electrical stimulation through optimal state transitions. *Cell Rep.* **28**, 2554–2566.e7 (2019).
24. G. Yan *et al*., Network control principles predict neuron function in the Caenorhabditis elegans connectome. *Nature* **550**, 519–523 (2017).
25. S. Gu *et al*., Optimal trajectories of brain state transitions. *Neuroimage* **148**, 305–317 (2017).
26. E. J. Cornblath *et al*., Temporal sequences of brain activity at rest are constrained by white matter structure and modulated by cognitive demands. *Commun. Biol.* **3**, 261 (2020).
27. T. M. Karrer *et al*., A practical guide to methodological considerations in the controllability of structural brain networks. *J. Neural Eng.* **17**, 26031 (2020).
28. S. W. Oh *et al*., A mesoscale connectome of the mouse brain. *Nature* **508**, 207–214 (2014).
29. W. Francesconi *et al*., Opiate dependence induces cell type-specific plasticity of intrinsic membrane properties in the rat juxtacapsular bed nucleus of stria terminalis (jcBNST). *Psychopharmacology (Berl.)* **234**, 3485–3498 (2017).
30. M. Hearing, Prefrontal-accumbens opioid plasticity: Implications for relapse and dependence. *Pharmacol. Res.* **139**, 158–165 (2019).
31. Y. Shen, X. Cao, C. Shan, W. Dai, T.-F. Yuan, Heroin addiction impairs human cortical plasticity. *Biol. Psychiatry* **81**, e49–e50 (2017).
32. O. Levran *et al*., Synaptic plasticity and signal transduction gene polymorphisms and vulnerability to drug addictions in populations of European or African ancestry. *CNS Neurosci. Ther.* **21**, 898–904 (2015).
33. D. E. Muskiewicz, G. R. Uhl, F. S. Hall, The role of cell adhesion molecule genes regulating neuroplasticity in addiction. *Neural Plast.* **2018**, 9803764 (2018).
34. N. Vogt, Optogenetic inhibition. *Nat. Methods* **17**, 29 (2020).
35. A. Pascual-Leone, V. Walsh, J. Rothwell, Transcranial magnetic stimulation in cognitive neuroscience–Virtual lesion, chronometry, and functional connectivity. *Curr. Opin. Neurobiol.* **10**, 232–237 (2000).
36. J. Silvanto, N. G. Muggleton, New light through old windows: Moving beyond the "virtual lesion" approach to transcranial magnetic stimulation. *Neuroimage* **39**, 549–552 (2008).
37. R. Z. Goldstein, N. D. Volkow, Drug addiction and its underlying neurobiological basis: Neuroimaging evidence for the involvement of the frontal cortex. *Am. J. Psychiatry* **159**, 1642–1652 (2002).
38. G. Di Chiara, A. Imperato, Drugs abused by humans preferentially increase synaptic dopamine concentrations in the mesolimbic system of freely moving rats. *Proc. Natl. Acad. Sci. U.S.A.* **85**, 5274–5278 (1988).
39. T. E. Robinson, K. C. Berridge, The neural basis of drug craving: An incentive-sensitization theory of addiction. *Brain Res. Brain Res. Rev.* **18**, 247–291 (1993).
40. L. D. Langlois, F. S. Nugent, Opiates and plasticity in the ventral tegmental area. *ACS Chem. Neurosci.* **8**, 1830–1838 (2017).
41. S. N. Haber, Corticostriatal circuitry. *Dialogues Clin. Neurosci.* **18**, 7–21 (2016).
42. L. M. Yager, A. F. Garcia, A. M. Wunsch, S. M. Ferguson, The ins and outs of the striatum: Role in drug addiction. *Neuroscience* **301**, 529–541 (2015).
43. S. B. Taylor, C. R. Lewis, M. F. Olive, The neurocircuitry of illicit psychostimulant addiction: Acute and chronic effects in humans. *Subst. Abuse Rehabil.* **4**, 29–43 (2013).
44. D. G. Winder, R. E. Egli, N. L. Schramm, R. T. Matthews, Synaptic plasticity in drug reward circuitry. *Curr. Mol. Med.* **2**, 667–676 (2002).
45. S. E. Hyman, R. C. Malenka, E. J. Nestler, Neural mechanisms of addiction: The role of reward-related learning and memory. *Annu. Rev. Neurosci.* **29**, 565–598 (2006).
46. E. E. Bagley, M. B. Gerke, C. W. Vaughan, S. P. Hack, M. J. Christie, GABA transporter currents activated by protein kinase A excite midbrain neurons during opioid withdrawal. *Neuron* **45**, 433–445 (2005).
47. J. Z. Kim, D. S. Bassett, Linear dynamics & control of brain networks. arXiv:1902.03309 (8 February 2019).
48. J. Schindelin *et al*., Fiji: An open-source platform for biological-image analysis. *Nat. Methods* **9**, 676–682 (2012).
49. A. Zalesky, A. Fornito, E. Bullmore, On the use of correlation as a measure of network connectivity. *Neuroimage* **60**, 2096–2106 (2012).
50. T. Wei, V. Simko, R package "corrplot": Visualization of a correlation matrix (Version 0.84, 2017).
51. G. Csárdi, T. Nepusz, The igraph software package for complex network research. *Complex Syst.* **2006**, 1695 (2006).
52. R Core Team, R: A language and environment for statistical computing (R Foundation for Statistical Computing, Vienna, Austria, 2013).
53. T. M. J. Fruchterman, E. M. Reingold, Graph drawing by force-directed placement. *Softw. Pract. Exper.* **21**, 1129–1164 (1991).
54. L. Dall'Asta, A. Barrat, M. Barthélemy, A. Vespignani, Vulnerability of weighted networks. *J Stat Mech: Theory Exp* **2006**, P04006 (2006).
55. F. Pasqualetti, S. Zampieri, F. Bullo, Controllability metrics, limitations and algorithms for complex networks. *IEEE Trans. Control Netw. Syst.* **1**, 40–52 (2014).
56. A. E. Motter, Networkcontrology. *Chaos* **25**, 97621 (2015).